==================== **MATHEMATICAL MODELING** ====================

UDK 530.1: 537.226.33: 541.1: 577.3

Modeling and Synchrotron Data Analysis of Modified Hydroxyapatite Structure

Bystrova A.V.[1,2]*, Dekhtyar Yu.D.[2], Popov A.I.[3,4], Bystrov V.S.[5]**

[1]Institute of Theoretical and Experimental Biophysics RAS, 142290, Pushchino, Russia
[2]Biomedical Engineering and Nanotechnology Institute, Riga Technical University, LV-1658, Riga, Latvia
[3]Institute M. von Laue - P.Langevin, 6, rue Jules Horowitz, Grenoble, France
[4]Institute of Solid State Physics, Latvian University, LV-1063, Riga, Latvia
[5]Institute of Mathematical Problems of Biology RAS, 142290, Pushchino, Russia

Abstract. The results are based on the first principal modeling and calculations for hydroxyapatite (HAP) nanostructures as native as well surface modified, charged and having various defects (H and OH vacancies, H internodes). HAP structures having being studied using Local Density Approximation (LDA) method with calculations of Density of States (DOS) allow us analyzing the experimental forbidden energy gap (Eg) and work function data. Molecular modeling by HyperChem is confirmed by photo-electron monochromatic measurements up to 6 eV and photo-luminescence (PL) data from synchrotron DESY experimental data up to 30 eV values. Brief analysis of the influence of heating, microwave radiation, hydrogenation, x-rays and synchrotron radiation on HAP surface is presented in this work. New data of the structure of modified hydroxyapatite are obtained. The determined energy levels for H internodes is $E_{H\text{-int}} \sim E_v + (1.5\text{–}2.0)$ eV, while for OH vacancy energy is in the range of $E_{OH\text{-vac}} \sim E_v + (2.9\text{–}3.4)$ eV inside the forbidden zone Eg. The analysis of PL emission allows us to conclude that these energies are close to observed main PL spectral line 420 nm (2.95 eV), and consequently OH vacancy could play the leading role in the surface energy levels changes and charging. But the influence of the inserted hydrogen is revealed too through excitation from most deep valence band levels due to existence of close overlapped molecular orbital with phosphorus atoms in the excited states. Both defects are observed by PL emission spectrum under synchrotron excitation energy in diapason ~8.5–14.5 eV.

Key words: hydroxyapatite, modeling, DOS, work function, photo-electron and photo-luminescence, defects: vacancies and internodes.

INTRODUCTION

Hydroxyapatite (HAP) is one of the most demanded materials in implantology of bones and teeth [1–5]. The main usage area is HAP coating on bone and dental implants to modify their surface properties for the best osseointegration [1, 2]. Biological HAP differs from the mineral one: it consists of many deviations such as non stoichiometry content, replacements, vacancies and other defects. As it was established from several early experimental works, and from our previous work (such as project PERCERAMICS [5]), interaction between HAP biomaterials and living cells (particularly, such as osteoblasts) is improved if the HAP surface is charged, or polarized [4, 5]. This data is confirmed by further studies of charged

---

HAP [6, 7], and additionally it was established that HAP surface geometry is influenced on the interactions with living cells [4, 7]. The influence of environments (pH index, citrate content, etc.) was established too [3, 8] as well as the variations of HAP nanoparticle size and shape in interactions with living cells [3, 4, 7, 8]. However, many unclear details of the mechanism remain as for formation of the surface charges, as well as of the interaction between electric charges, surface potential and living cells (osteoblasts and other osteo-cells leading to bone tissues formation) on the HAP surface. Some attempts and results using first principle Local Density Approximation (LDA) and Density of States (DOS) calculations were presented recently in [9]. We consider here some further calculations for surface modified HAP interacting with living cells based on this approach. The aim of this work was to look deeper levels of electron excitation of hydroxyapatite for more clear understanding of its deepest structure and influence on such defects as vacancy and inter-node, especially of hydrogen atoms (protons) as well as the hydroxyl groups (OH). The available photoelectron excitation technique, that we have, allows us to see the result of usual excitation only at the levels up to 6 eV. Synchrotron technique gives us an opportunity to see and study the electron excitations up to 35 eV. As HAP is widely used, it is necessary to study its properties under the influence of various factors to predict the behavior inside living structures.

MAIN INPUT DATA AND SUPPOSITIONS

Computational Methods and Models

In this work we use calculations by density functional theory (DFT) at local density approximation (LDA) [9]. We use the standard valence configurations for hydrogen ($1s_1$), for phosphorus ($3s_2 3p_3$) and for oxygen ($2s_2 2p_4$). But for calcium we use two different valence configurations: 1) Ca2 with 2 valence electrons ($4s_2$) shell, and most accurate 2) Ca10 with 10 valence electrons ($3s_2\_3p_6\_4s_2$) shell. The cutoff for the kinetic energy for bulk calculations was at the 300 atomic unit of energy (a.u., 1 a.u. ~ 27.2114 eV). The Monkhorst–Pack k-point meshes for the Brillouin Zone (BZ) integration of hexagonal and monoclinic primitive cells were found that the best are $2 \times 2 \times 4$. The initial lattice unit cell for hexagonal HAP structure consists of 44 atoms, while for monoclinic HAP nanostructures it consist of 88 atoms, because the lattice unit cell is doubled in this last monoclinic case along b axis. For super-cell model calculations we use 88 and 176 atoms consequently. In all calculations — except the elastic constant calculations — we allow full relaxation of the cell, including changing the volume and adjusting the atomic positions and cell shape.

Firstly, we constructed lattice unit cell models as for hexagonal HAP phase as well as for monoclinic phase. We use modeled and computed data from our previous HAP nano-particle models [3] as first approximations for lattice unit cell. The experimental data was used from [10, 11] as well as data of calculations from [11–13]. Several of new computed and used here data was published recently in our paper [14].

Used Experimental Methods and Materials

Initially, 12 samples of HAP (preliminary fabricated before this study as described in [5]) were selected randomly. The following scheme of investigation was applied to them. First, the photo-emission spectrum of each sample was measured using equipment, assembled from MSD-2 monochromator, a vacuum chamber from KURT J. LESKER, Geigerzähler Dosimeter Strahlenmessgerät Robotron 20046 (dosimeter Geiger Robotron 20046). Subsequently, to the different samples different processing treatment scheme was applied as shown on the picture below (Fig. 1). Two samples were control samples without any treatment.

The heating was held for 30 minutes at the temperature interval of 542–546ºC and under pressure of (7.5–8.7)*10^{-6} Pa, which was obtained at a rate of 15 degrees per minute. The

hydrogenation was carried out for 6 hours at settings 60 ± 2 atmospheres, $t = 23^{\circ}$C. The power of applied microwave radiation was 800 W and this treatment of the samples was carried out for $t = 6.5$ min. The ionizing radiation was applied at a dose of 1MGray. Irradiation by γ-rays with energy of 18 MeV was applied at a dose flow 10 Gray/min.

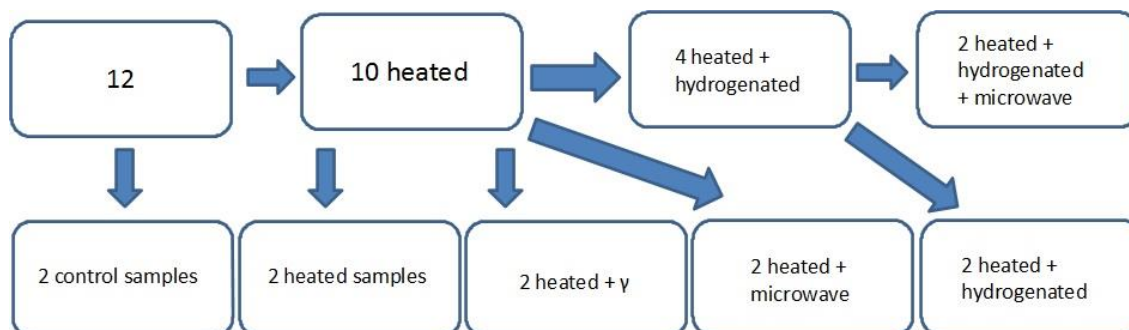After all performed influences a control measurement of the photo-emission spectrum was conducted again.

Figure 1. Scheme of HAP samples processing.

Then, all samples were sent to the group of Dr. A. Popov for synchrotron irradiation studies on DESY (Deutsches Elektronen-Synchrotron, Hamburg). Some samples were selected randomly and were looked at different wavelengths in the case of excitation and photo-luminescence (PL) emission. Firstly, we try to find the most important PL emission spectral line after initial excitation with 180 nm wave length, corresponding to energy 6.89 eV, which is much greater than all known data of energy of HAP forbidden zone gap width $Eg = Ec - Ev$, where Ec is conductance band bottom and Ev is valence band top (see below, Fig. 6). Consequently, excited electrons from valence band jump up to conductance band (and create electron-hole pairs), where electrons relax to the bottom of the conductance band and then fall down onto some energy trap levels Ei inside Eg with emission of photons having certain energy $\Delta Ei = h\nu = hc/\lambda = Ec - Ei$ – with corresponding wave length λ and frequency ν (where h is Plank constant and c is light velocity). Second, after determination this energy Ei and PL wave length, we conduct registration of PL emission spectra at this spectral line, during performing the excitation of samples from synchrotron irradiation in full energy diapason approximately $\lambda = 333$–80 nm (or energy 3.72–15.5 eV). After bringing samples back, their photo-emission spectrum was measured again by the above described technique.

MAIN OUTPUT DATA, RESULTS AND DISCUSSIONS

Experimental data and results

After performing of all experimental works we made the processing of all observed data to find the most essential and impact results. Having reviewed the entire data set after treatment effects on HAP, we can find for the derivative and its approximation up to 30 points, showing the intensity of radiation as a function of wavelength, the peaks everywhere in the range 5.5–5.9 eV, corresponding to work function values of usual bulk HAP crystal. It is the relative number of fluorescent photons in wavelength dependence. We also evaluated the effects of various treatment factors, described above. For example, a variation of common effects of hydrogenation, microwave radiation and heating processes are presented on Fig. 2.
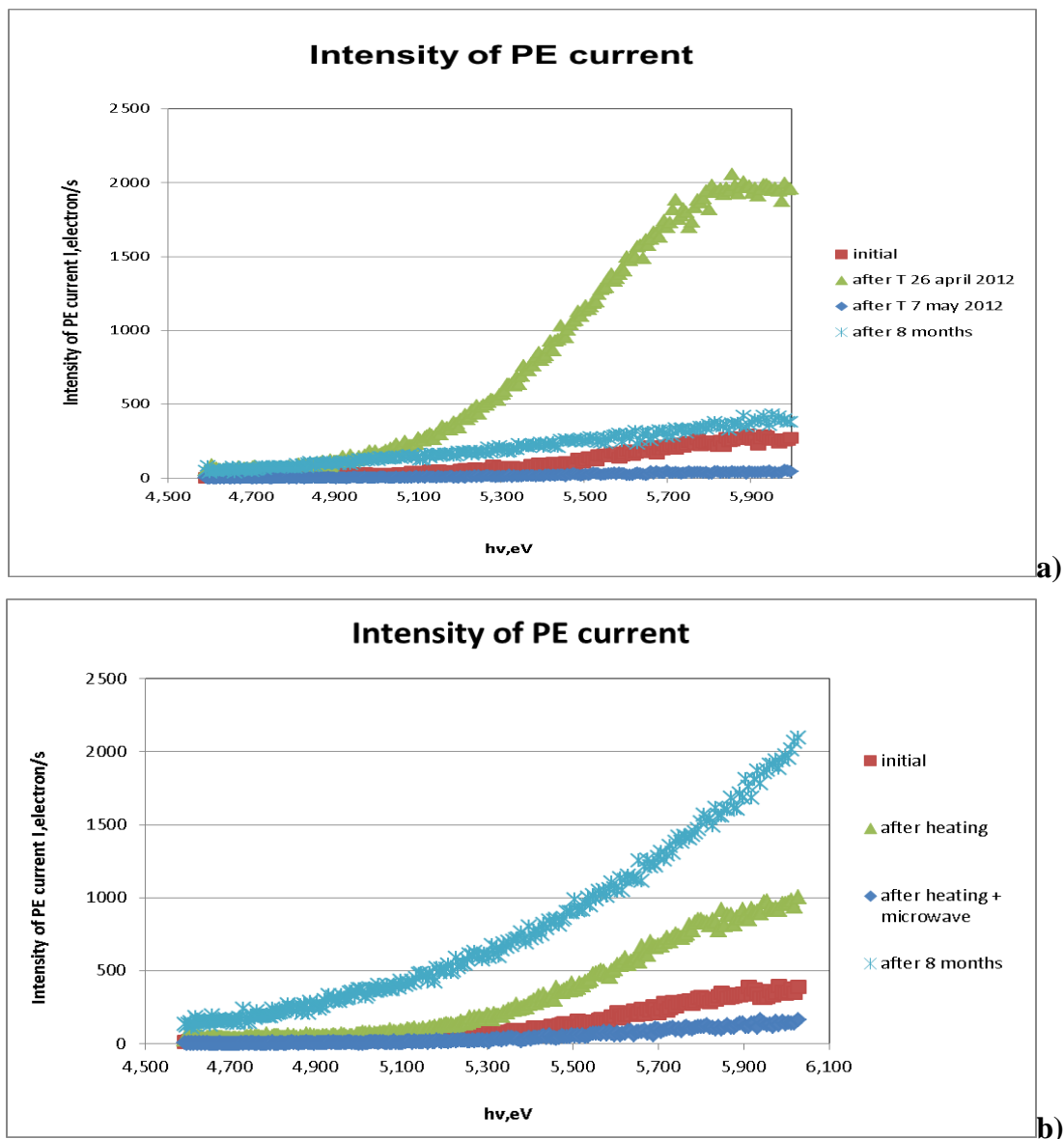
173

Figure 2. The influence of heating (a) and microwave radiation (b).
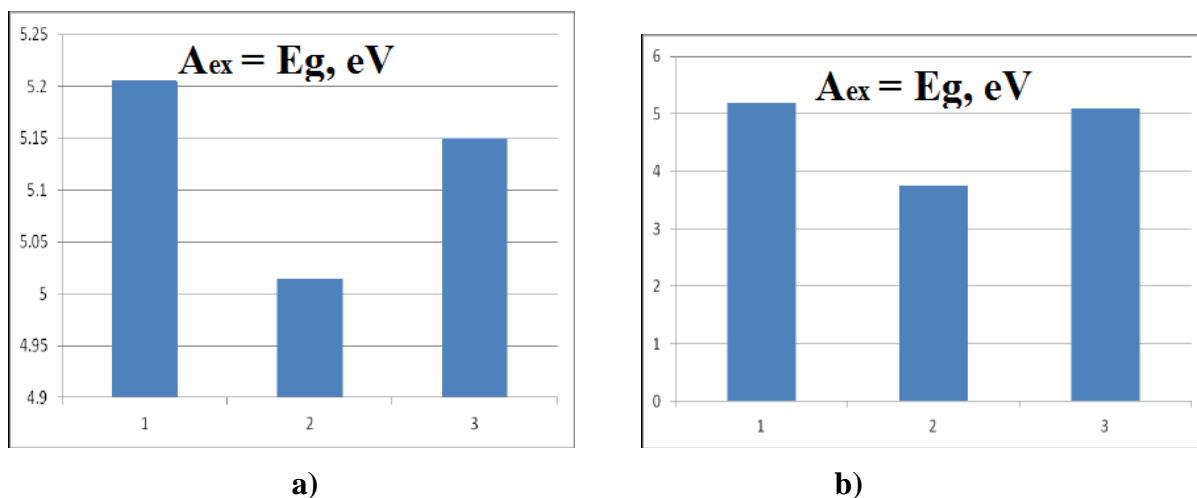

Figure 3. Values of the electron work function: 1 – the original electron work function *Aex* before any influences, 2 – after the applied effects such as microwave radiation, hydrogenation and heating, 3 – after the synchrotron radiation.

174

The corresponding variations of electron work function *Aex* are presented on Fig. 3. In general, the variations of *Aex* are around values: 5.25 eV for case 1; 5.04 eV for case 2 and 5.24 eV for case 3. However, after some treatment (e.g., heating/microwave) *Aex* was ~ 3.75 eV. But the main result was obtained from the synchrotron spectrum after heating and microwave irradiation, and some after hydrogenation of HAP (Fig. 4, Fig. 5).
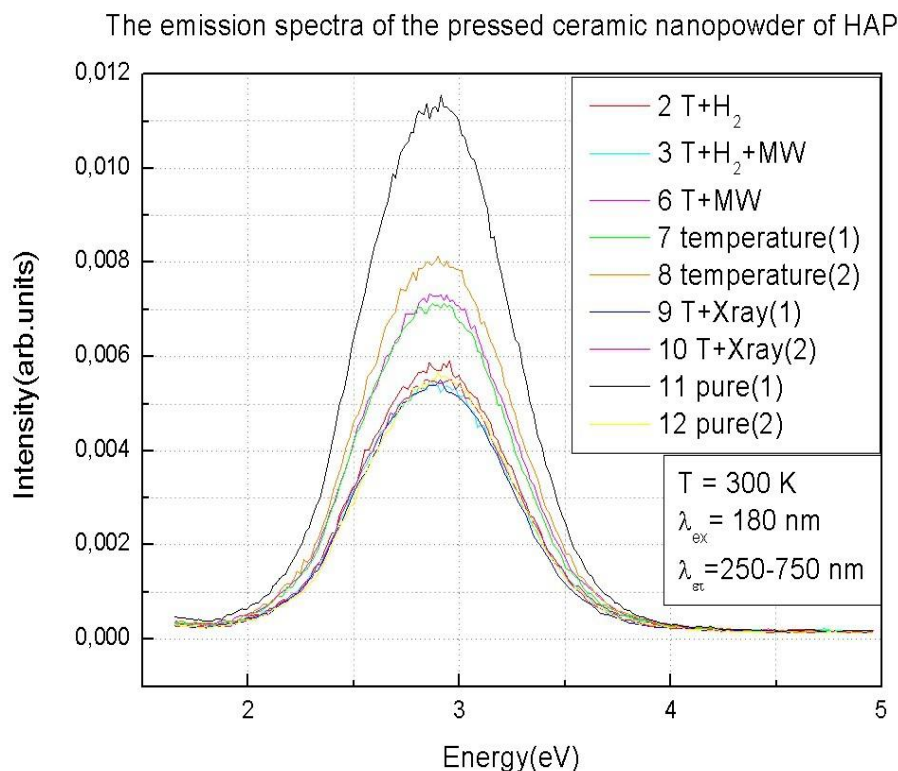

Figure 4. Data of the synhrotron emission PL spectrum.

It follows from the obtained data for initial emission PL spectrum (Fig. 4) that for all kinds of the sample's treatments there is only one main PL energy level with energy $Ei = \sim$ 2.95 eV (or with wave length ~420 nm). But the main rises of intensity for this energy level are after heating, heating with Xray, heating with microwave irradiation and with hydrogen (see curves 7, 8, 10, 6, 3 on the Fig. 4.). This result means that after corresponding treatments of the samples we obtain rise of some defects in the HAP samples, which have recombinant energy level in the forbidden zone with value $Ei \sim 2.95$ eV ~ 3 eV (or 420 nm line) from the bottom of conductance band. We suppose that the origin of this defect might be both OH vacancy and H internodes. Corresponding rise of intensity for the treatments is 27–45%.
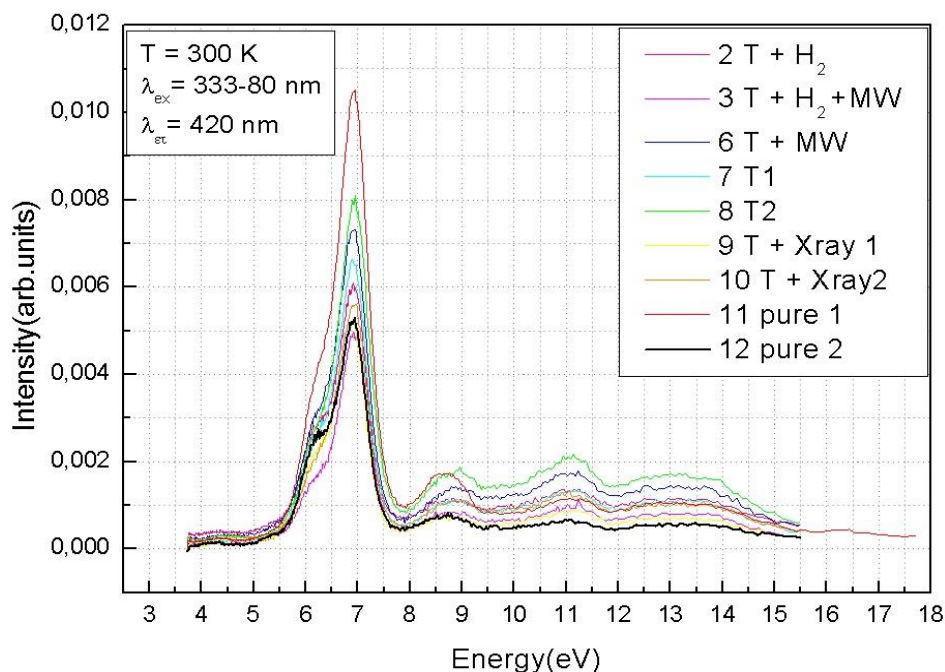
After that measurements of the excitation PL spectrum in all energy diapason from 4 up to 20 eV were performed for this 420 nm line. Figure 5,a shows the total obtained spectrum, while on Fig. 5,b details of high energy spectrum from 8 up to 20 eV are presented.

It is well known, that HAP formula is $Ca_5(PO_4)_3(OH)$. Conducted preliminary analysis leads to the following conclusion that the observed at high energies peaks at ~ 9–10.5, 11–12, 13–14 eV can match most likely the 1st ionization potential (IP) of the phosphorus atom P (which is close to the isolated atom with the value ~ 10.5 eV), the 2nd IP of the calcium atom Ca (which is ~ 11.87 eV for the isolated atom, while 1st IP ~ 6 eV is usually close to the forbidden zone of HAP crystal) and 1st IP of the oxygen atom (which is ~ 13.6 eV for isolated atom). This last value is also corresponding to the IP ~ 13.6 eV of the isolated hydrogen atom.

From the calculations of the density of state (DOS) for HAP crystal it is known [9, 13] that these energy peaks for the first P 3s and P 3p orbitals, Ca 3D+4S orbitals, O 2P orbitals and H 1S orbitals have approximately the same energies as reckoned from the bottom of conductive band, taken into account that registered at our experiments excited electrons from
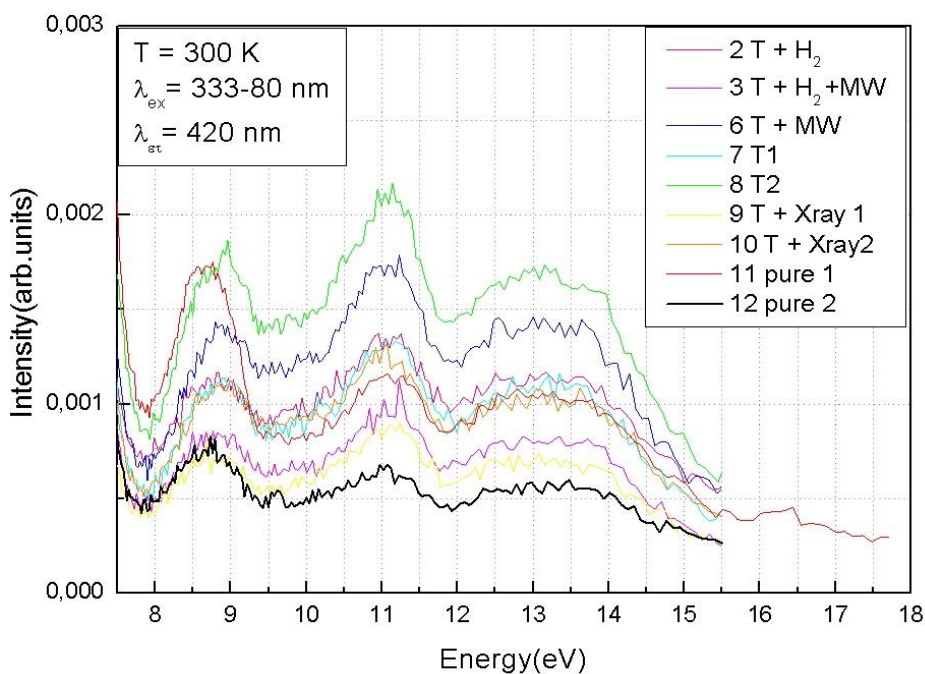
175

valence band fall to the bottom of the conduction band through the forbidden energy band gap, equal to *Eg* ~ 5.2–5.9 eV. Thus, the obtained energy differences are at the same order of the magnitudes for the excitation of electrons from these orbitals of the HAP. This conclusion requires detailed examination and this issue is in the course of our further work. Below we consider some of our proposed models, calculations and interprations of obtained data.

a)

b)

Figure 5. Data of the synchrotron excitation spectrum for 420 nm: a) total, b) high energy.

176

Computational models, data, discussion and analysis

Firstly, one of the most important computational results is that for the monoclinic cell the total cell energy is equal –934.20024 a.u. It is equal to –467.10012 a.u. , which is a ½ from this value for corresponding hexagonal primitive unit cell. It is lower than the total energy of the unique hexagonal cell (for directly computed hexagonal total energy = – 467.09923 a.u.) on the value ΔE = 0.00089 a.u.= 0.024218 eV ~ 24.2 meV. This result is comparable with [12], where the similar result is ~ 22 meV, and confirms the data about possible co-existence of monoclinic and hexagonal HAP phase at the room temperature. More details and discussions of these calculations are presented in [9, 14].

Secondly, the other important result is that we calculated the DOS distributions for initial optimized HAP lattice and for all atoms positions. We obtained the data of the forbidden gap Eg [9, 14], which is very close to the known data, but we have variations with used approximation of model (~ 5.44 eV for model 10 Ca electrons Ca10 shell, in comparison with ~ 5.68 eV for model Ca2 shell) [9, 14]. Calculation of DOS allow us to study also the influence of lattice's charges on the shift and changes of Eg, which are in good correlations with experimental data on living cells attachment to charged HAP surface [3, 6–9].

The question is arisen – what is the nature of these surface charges? Experimentally, it was possible to create an excess charge in the surface layers of the HAP, by placing the sample in a chamber filled with hydrogen at high pressure. This process is named *hydrogenation* [7]. We suppose that during the hydrogenation process the inserted hydrogen atoms could create both interstitial/internodes and well vacancies (O or OH types). But, heating and microwave irradiation also could give an opportunities for protons jump through OH-channels energy barriers inside HAP surface layers [4].We calculated DOS for initial HAP state and with several defects. For pure HAP structure (Fig. 6) we obtained only shifts of DOS energy levels with change of cell unit charge [9].
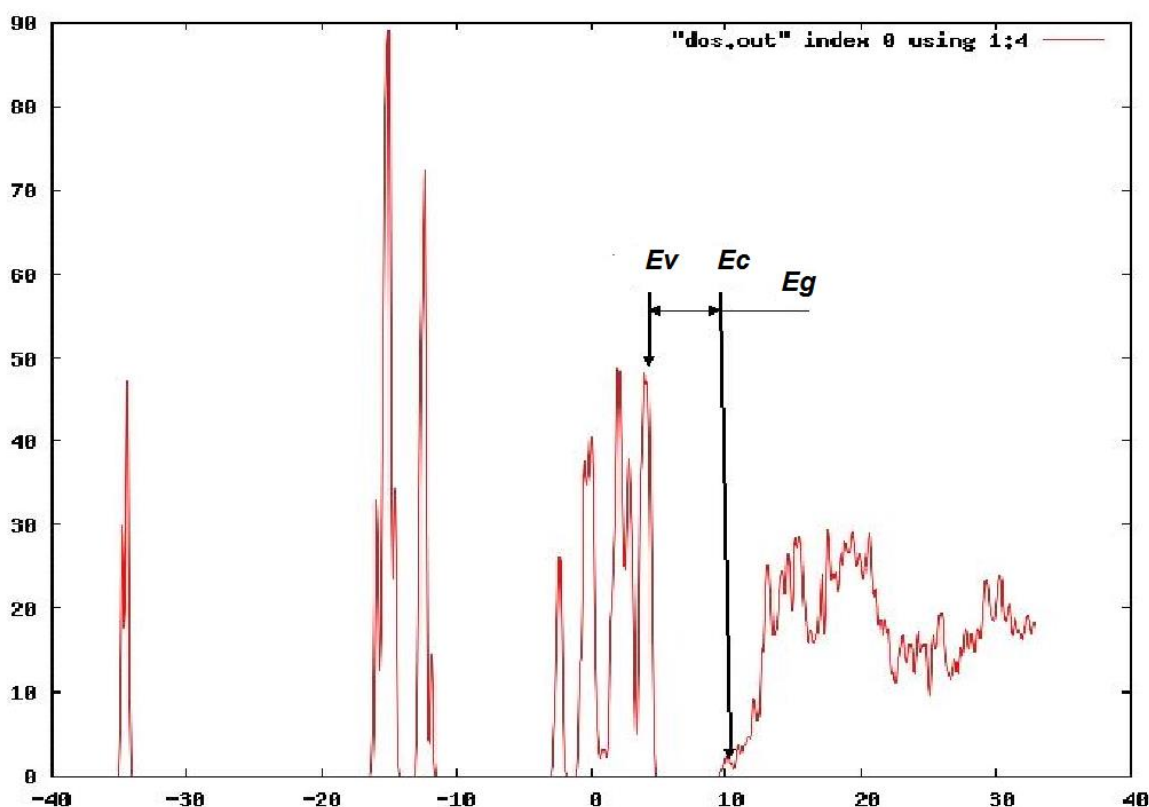

Figure 6. DOS for initial pure hexagonal HAP structure.

177

It is interesting, that if one excess hydrogen is introduced per one unit cell (e.g., for hexagonal phase with LDA Ca2 model), we obtain beyond small shift of all energy levels the arising of the strong additional energy levels inside of the forbidden zone E_g with energy approximately 1.5…2 eV from the top of the valence band: $E_{H-int} = \sim E_v + 1.5...2.0$ eV (Fig. 6). It is H internodes energy trap level.
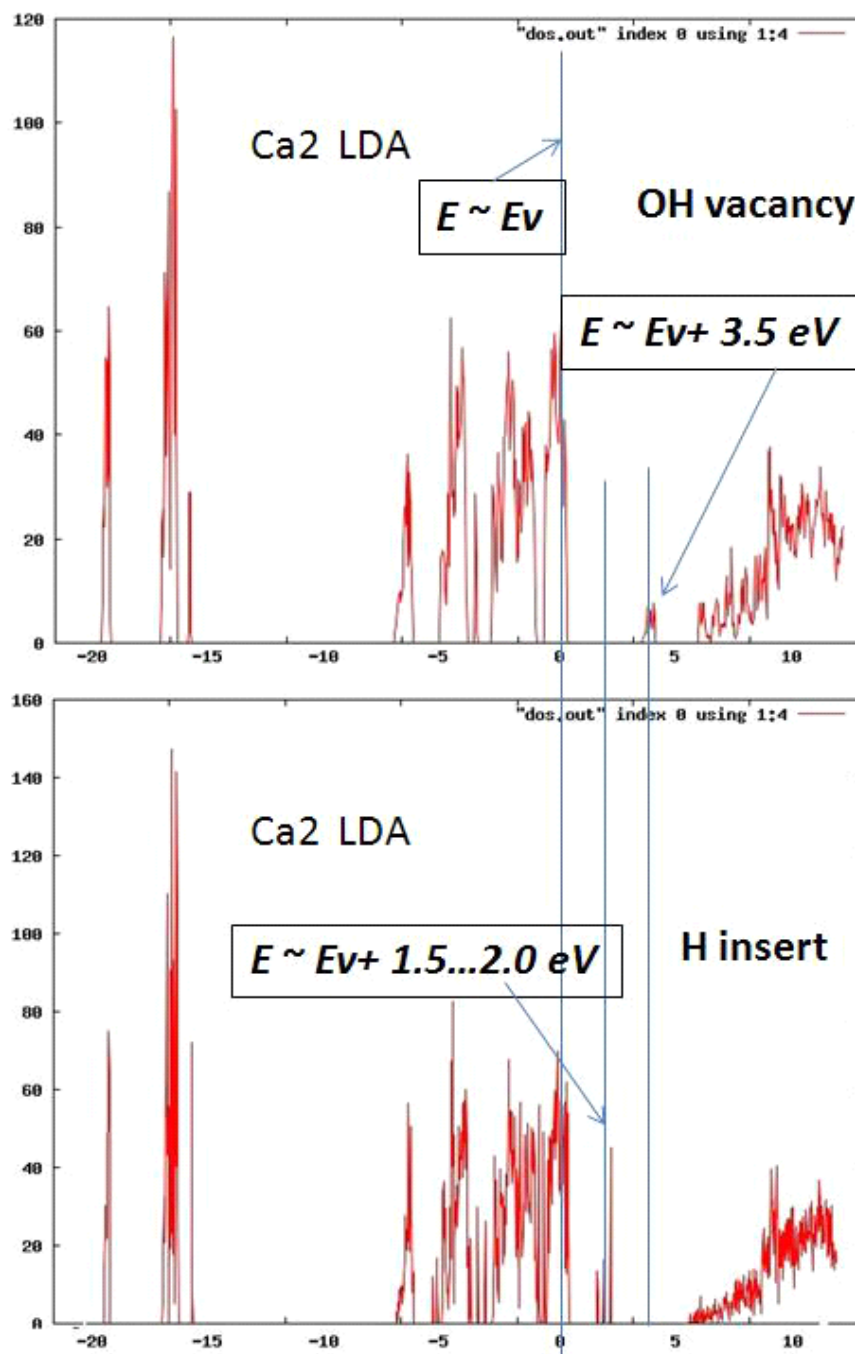

Figure 7. DOS from HAP structure with one OH vacancy and one excess inserted hydrogen atom H.

For vacancy of one hydrogen atom we obtain additional energy level, which is very close to the top of valence band: $E_{H-vac} = \sim E_v + 0.2$ eV. But for OH vacancy we obtain deep energy level: $E_{OH-vac} = E_v + 3.5$ eV, which is more close to the bottom of conductive band (Fig. 7). Moreover there is also some narrow band between energies of $E_{OH-vac} = E_v + (2.9 - 3.4)$ eV. These last results are very close to the data in [13, 14]. It is interesting that in work [15] the surface level with energy $E5 = Ev + 3.3$ eV is very close to values $Ev = Ev + (2.9 - 3.4)$ eV,

which was observed experimentally. It is important that the used HAP samples had *p*-type semiconducting property, confirmed that it is recombinant hole levels, which trapped electrons from the conductive band. As a result we obtain the PL emission, when electrons are trapped by this level. But the nature of this surface level was not clear. Authors [15] suppose that it might be OH vacancies, which could rise after heating. Now we can confirm that it must be OH-vacancy in the HAP surface layer. The rise of PL intensity at the 11 eV is in the range 3–3.7 times for heating (8 T2) and heating with microwave (6 T + MW), that is close to [15] for OH annealing.

Another important model might be connected with inserted proton into HAP structure {a proton inserted into HAP structure} through OH-channel. In this case we obtain the overlapped orbitals, which could serve as some intermediate state for further electron transitions from the excited state to the trapped one.

We elaborate this model of one inserted H atom in HAP unit cell (Fig. 8) and after optimization of total unit cell structure and positions for all atoms we obtain that this atom H is positioned very close to atom P.
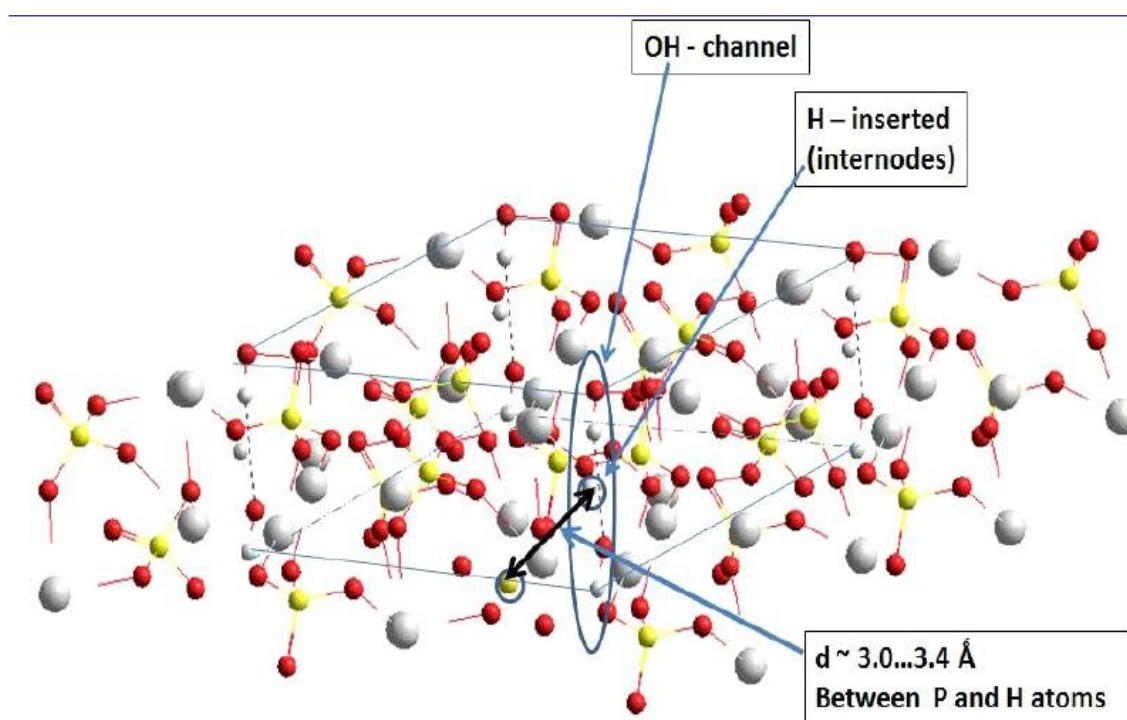

Figure 8. Model of hexagonal HAP with inserted one extra H.

In this case after excitation (using, for example, synchrotron irradiation) with $E > Eg$, the excited electron, which jumps from orbitals in the valence band up to the excited high molecular orbital (which is empty before excitation and therefore named as Low Un-Occupied Molecular Orbital: LUMO), could exist in the joined or overlapped molecular orbitals between atoms H and P (Fig. 9).

As a result, after relaxation electrons fall down from this LUMO (it is excited state) on HOMO 1 (Highest Occupied Molecular Orbital 1), of P atom, from which electrons were excited before (or it might be another orbital in valence band), during influence of the large synchrotron energy (~ 6–30 eV). The finally resulted electron trapping process leads to PL emission having the final energy with total issuance of the order ~ 8 eV...~ 14 eV (Fig. 10),

179

that is close to the obtained experimental data and are in the same energy range values. This model is confirmed by PL emission intensity rise by ~ 2 times in 11 eV range for treatment with hydrogenation (2 T + H2) (see on Fig. 5,b). These proposed models and obtained results require further development and are in the focus of our next work.
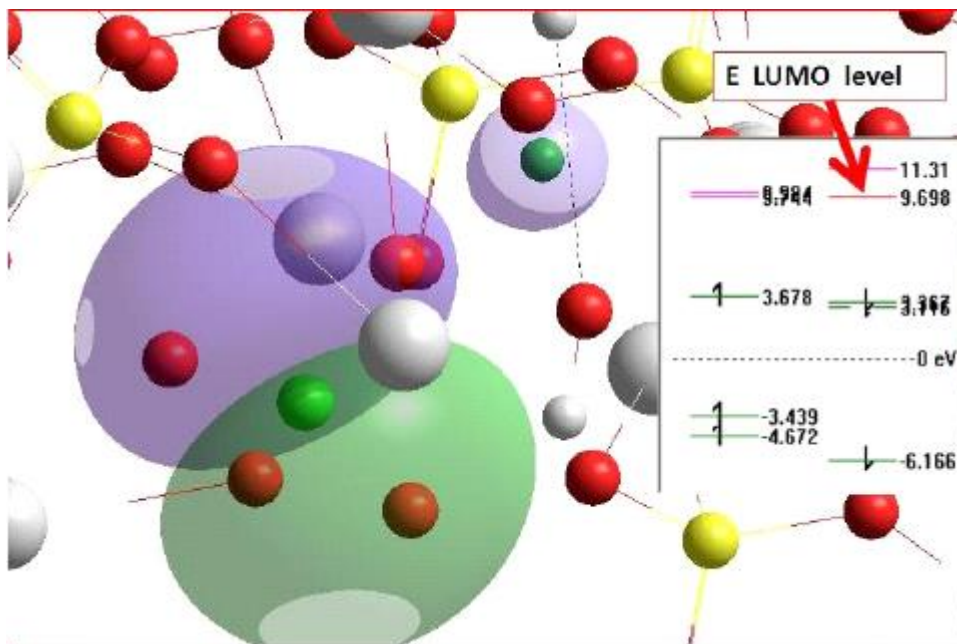

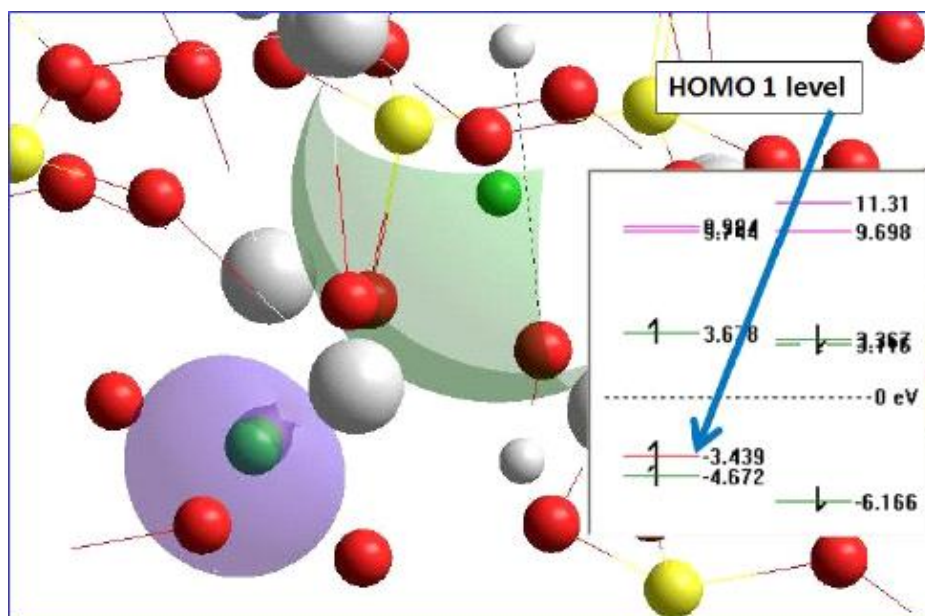**Figure 9.** Overlaping of excited electron molecular orbitals LUMO of the atoms H and P.

Figure 10. Energy issue of electron cascade relaxation process.

180

CONCLUSIONS

1. The computational technique for first principle calculations of the HAP structures was developed using LDA DFT methods and applied for calculations in pure hexagonal and monoclinic HAP phases as well as for HAP structure's defects.

2. The calculations of defects were performed for hydrogen vacancy and internodes, as well as for OH vacancy. Calculated DOS show the arising of energy levels $E_{\text{H-}int} \sim Ev + (1.5\text{-}2.0)$ eV for H inter-node and narrow bands $E_{\text{OH-}vac} \sim E_v + (2.9\text{–}3.4)$ eV for OH vacancy inside the forbidden zone Eg.

3. Computed data show that monoclinic phase with opposite oriented OH ions in the neighboring channels have lowest energy on ~24 meV for Ca2 model and on ~ 2 meV for Ca10 model in comparison with hexagonal HAP ordered phase.

4. Obtained data on HAP after temperature and microwave treatments show the rise of the PL emission peak at ~ 2.95 eV (420 nm) and, then, series of the PL peaks (~ 9 eV, 11 eV, 13 eV) at this PL line after synchrotron excitation in the interval from 4 up to 20 eV. These peaks are explained by excitation from orbitals in valence band as follows from developed model and calculations of the DOS. The intensity of these peaks <u>rises</u> after heating and microwave irradiation too, that correspond to rise of the OH vacancy defects following the developed model. Another model proposes that the rise of these peaks might be explained by models of the interacting between additionally inserted H, which was arisen in the close position to P atom with overlapped electron wave functions for excited electron states. During following electron relaxation and final trapping on the $E_{\text{OH-}vac}$ PL emission with ~ 420 nm is observed.

5. Finally, all these data could be very useful for further development of technological control of the annealed OH vacancies and inserted H during HAP treatment and other wide practical applications, which are necessary for HAP surface modification such as its electrical charging.

REFERENCES

1. Epple M., Ganesan K., Heumann R., Klesing J., Kovtun A., Neumann S., Sokolova V. *J. Mater. Chem.* 2010. V. 20. № 1. P. 18–23.
2. Ratner B.D., Hoffman A.S. *Biomaterial Science*. London: Academic Press, 1996.
3. Bystrov V.S., Paramonova E., Dekhtyar Yu., Katashev A., Karlov A., Polyaka N., Bystrova A.V., Patmalnieks A., Kholkin A.L. Computational and experimental studies of size and shape related physical properties of hydroxyapatite nanoparticles. *J. Phys.: Condens. Matter*. 2011. V. 23. P. 065302.
4. Bystrov V.S., Bystrova N.K., Paramonova E.V., Dekhtyar Yu.D. Interaction of charged hydroxyapatite and living cells. I.Hydroxyapatite polarization properties. *Mathematical biology and bioinformatics*. 2009. V. 4. № 2. P. 7–11.
5. *PERCERAMICS: Multifunctional percolated nanostructured ceramics fabricated from hydroxyapatyte* (NMP3-CT-2003-504937 FP6 project): Final Report Summary. URL: http://cordis.europa.eu/result/report/rcn/51676_en.html.
6. Dekhtyar Yu., Polyaka N., Sammons R. *IFMBE Proceedings*. 2008. V. 20. P. 23–25.
7. Dekhtyar Yu., Bystrov V., Bystrova A., Dindune A., Katashev A., Khlusov I., Palcevskis E., Paramonova E., Polyaka N.N., Romanova M., Sammons R., Veljović D. *IFMBE Proceedings*. 2013. V. 38. P. 182–185.
8. Martins M., Santos C., Almeida M., Costa E. *J. Coll. & Interface Sci*. 2008. P. 210–216.
9. Bystrov V., Costa E., Santos S., Almeida M., Kholkin A., Dekhtyar Yu., Bystrova A.V., Kopyl S., Paramonova E.V. Computational study of hydroxyapatite properties and surface interactions. *IEEE Conf. Publications*. 2012. P. 1–3.
10. Mostafa N.Y., Brown P.W. *J. Phys. Chem. Solids*. 2007. V. 68. P.431.

11. Tofail S.A.M., Harvety D., Stanton K.T., McMonagle J.B. Structural order and dielectric behaviour of hydroxyaopatite. *Ferroelectrics*. 2005. V. 319. № 1. P. 117–123.

12. Slepko A., Demkov A.A. First-principles study of biomineral hydroxyapatite. *Phys. Rev. B*. 2011. V. 84. P. 134108.

13. Matsunaga K., Kuwabara A. First-principles study of vacancy formation in hydroxyapatite. *Phys Rev B*. 2007. V. 75. P. 014102.

14. Bystrov V.S., Paramonova E.V., Costa M.E., Santos C., Almeida M., Kopyl S., Dekhtyar Yu., Bystrova A.V., Maevsky E.I., Pullar R.C., Kholkin A.L. A Computational Study of the Properties and Surface Interactions of Hydroxyapatite. *Ferroelectrics*. 2013. V. 249. P. 94–101. DOI: 10.1080/00150193.2013.822774.

15. Aronov D., Chaikina M., Haddad J., Karlov A., Mezinskis G., Oster L., Pavlovska I., Rosenman G. Electronic states spectroscopy of Hydroxyapatite ceramics. *J. Mater. Sci.: Mater. Med*. 2007. V. 18. № 5. P. 865–870.